

Global Biogeochemical Cycles®

RESEARCH ARTICLE

10.1029/2022GB007490

Key Points:

- A large-scale field survey and a global meta data set were conducted to investigate the effects of afforestation on soil N and C:N
- Afforestation increased soil C and N storage in N-poor soils but decreased them in N-rich soils
- Changes in soil C:N with afforestation were mediated by initial relative abundance of soil C and N and mycorrhiza type of planted trees

Supporting Information:

Supporting Information may be found in the online version of this article.

Correspondence to:

N. Cong and J. Ding,
congnan@igsnr.ac.cn;
jzding@itpcas.ac.cn

Citation:

Hong, S., Cong, N., Ding, J., Piao, S., Liu, L., Peñuelas, J., et al. (2023). Effects of afforestation on soil carbon and nitrogen accumulation depend on initial soil nitrogen status. *Global Biogeochemical Cycles*, 37, e2022GB007490. <https://doi.org/10.1029/2022GB007490>

Received 9 JUN 2022
Accepted 20 DEC 2022

Author Contributions:

Conceptualization: Songbai Hong, Shilong Piao, Lingli Liu, Anping Chen
Data curation: Songbai Hong, Nan Cong
Formal analysis: Songbai Hong
Funding acquisition: Shilong Piao
Investigation: Songbai Hong, Nan Cong, Jinzhi Ding
Methodology: Songbai Hong, Nan Cong, Shilong Piao
Project Administration: Shilong Piao
Supervision: Shilong Piao
Writing – original draft: Songbai Hong
Writing – review & editing: Songbai Hong, Nan Cong, Jinzhi Ding, Shilong Piao, Lingli Liu, Josep Peñuelas, Anping Chen, Timothy A. Quine, Hui Zeng, Benjamin Z. Houlton

© 2022. American Geophysical Union.
All Rights Reserved.

Effects of Afforestation on Soil Carbon and Nitrogen Accumulation Depend on Initial Soil Nitrogen Status

Songbai Hong¹ , Nan Cong² , Jinzhi Ding³ , Shilong Piao^{1,3} , Lingli Liu⁴ , Josep Peñuelas^{5,6} , Anping Chen⁷ , Timothy A. Quine⁸ , Hui Zeng⁹ , and Benjamin Z. Houlton¹⁰

¹College of Urban and Environmental Sciences, Sino-French Institute for Earth System Science, Peking University, Beijing, China, ²Key Laboratory of Ecosystem Network Observation and Modeling, Lhasa Plateau Ecosystem Research Station, Institute of Geographic Sciences and Natural Resources Research, Chinese Academy of Sciences, Beijing, China, ³Key Laboratory of Alpine Ecology and Biodiversity, Center for Excellence in Tibetan Earth Science, Institute of Tibetan Plateau Research, Chinese Academy of Sciences, Beijing, China, ⁴State Key Laboratory of Vegetation and Environmental Change, Institute of Botany, Chinese Academy of Sciences, Beijing, China, ⁵CREAF, Barcelona, Spain, ⁶CSIC, Global Ecology Unit CREAM-CSIC-UAB, Catalonia, Spain, ⁷Department of Biology, Graduate Degree Program in Ecology, Colorado State University, Fort Collins, CO, USA, ⁸Department of Geography, College of Life and Environmental Sciences, University of Exeter, Exeter, UK, ⁹Peking University Shenzhen Graduate School, Shenzhen, China, ¹⁰Department of Ecology and Evolutionary Biology, Department of Global Development, Cornell University, Ithaca, NY, USA

Abstract Long-term carbon (C) sequestration in terrestrial vegetation and soil is mediated by soil nitrogen (N) supply. Afforestation is regarded as a global-scale solution to climate change; thus, resolving the role of N in either facilitating or reducing the long-term C benefits of this practice has essential implications to maximize its C sink potential. The impacts of afforestation on soil C, N, and their stoichiometric ratio have been widely explored but what regulates these impacts remains unclear at regional and global scales. In this study, we conducted an intensive field sampling investigation including 610 pairs of afforested and control plots in northern China and extensively compiled a global data set containing 211 afforested-control pairs worldwide to evaluate responses of soil N concentrations and C:N ratios to afforestation and further explored their major regulator. We identified a soil N threshold, the inflection point where afforestation changes from increasing to decreasing soil C and N, which was 0.86 (95% CI: 0.81–0.91) kg N m⁻² in 0–1 m depth. Changes in soil C:N ratios with afforestation were mediated by initial relative abundance of soil C and N and types of mycorrhiza associated with planted trees. Increases in soil C:N were mostly driven by trees with ectomycorrhizal associations but did not change for those associated with arbuscular mycorrhizal fungi. These results provide a data-based understanding on soil C and N dynamics following afforestation and its underlying mechanisms and further highlight the importance of site selection based on initial soil properties in future afforestation.

Plain Language Summary The C sequestration potential of afforestation is largely regulated by soil N supply. However, how initial soil N status regulates soil C and N dynamics after afforestation remains poorly understood. In this study, we conducted a systematic field campaign from representative afforested areas in northern China and compiled a meta-data set at the global scale from 86 peer-reviewed papers to fill this knowledge gap. We found that afforestation increased soil C and N storages in N-poor soils but decreased them in N-rich soils. Changes in soil C:N ratios with afforestation were mediated by the initial relative abundance of soil C and N. Moreover, increases in soil C:N were mostly driven by trees with ectomycorrhizal associations but did not change for those associated with arbuscular mycorrhizal fungi. These findings provide a benchmark for evaluating the ecological benefits and costs of afforestation and also have implications for future afforestation site selection.

1. Introduction

Afforestation is becoming a global movement toward the combined benefits of ecological restoration and the mitigation of climate change (Bastin et al., 2019; IPCC, 2014). Although highly uncertain and controversial, global afforestation may have the potential to sequester as much as 205 Gt C, reducing the global burden of anthropogenic emissions of CO₂ by 68% (Bastin et al., 2019). A central unknown in such estimates depends on the role of supplies of soil nitrogen (N) and how this macronutrient could either facilitate or constrain decadal CO₂ sequestration via afforestation practices (Luo et al., 2004, 2006). N is principally an essential component of proteins and

nucleic acids, which controls the metabolism and reproduction of plants (Scheible et al., 2004). Photosynthesis, the process producing major inputs of carbon (C) to ecosystems, is usually limited by the supply of soil N, especially in temperate ecosystems (Luo et al., 2004, 2006). Soil N constraints may increase with afforestation because more soil N will be absorbed and locked into aboveground biomass (Berthrong et al., 2009). The ability of soils to store C is also linked to N; N influences the decomposition of organic matter via microbial regulation and is stoichiometrically linked to C within a narrow range (Mooshammer et al., 2014). Soil N accordingly plays a key role in modulating the input and output of C in ecosystems (Vries et al., 2006; Vries et al., 2009) and further regulates the C sequestration capacity of ecosystems (Niu et al., 2016; Vitousek et al., 1997).

Besides soil N stock, the stoichiometric ratio of C and N (C:N) also strongly regulates soil N supply and ecosystem C sequestration (Mooshammer et al., 2014; Vries et al., 2006; Vries et al., 2009). On the one hand, C:N can be used to indicate the N demand per unit of C storage; thus, an increase in C:N may indicate the enhanced C sequestration in the absence of concomitant increases in N supplies (Cotrufo et al., 2019). On the other hand, however, C:N also indicates the intensity of N limitation (Mason et al., 2022). Increased soil C:N indicates lower N availability and progressive N limitation (Luo et al., 2004; Mason et al., 2022), which would restrict future C sequestration (Vries et al., 2006; Vries et al., 2009). Therefore, exploring the changes of soil C:N after afforestation is important for understanding soil C and N interaction and predicting future C sink potential of planted forests.

The effects of afforestation on soil N and its stoichiometric ratio with C have been widely investigated in previous studies (Berthrong et al., 2009; D. Li et al., 2012; Xu et al., 2016). However, the impacts of afforestation on soil C and N showed large spatial heterogeneity (D. Li et al., 2012) with either positive (Lemma et al., 2006), negative (Farley et al., 2004), or negligible effects (Richter et al., 1999). It remains a puzzle why afforestation had such divergent impacts on soil C and N stocks in different regions. As shown in previous studies, the effects of afforestation could vary with climate zone, soil type and properties, planted tree species, stand age, and original vegetation types (Berthrong et al., 2009; D. Li et al., 2012). However, the major factors that regulate soil C and N dynamics after afforestation remain poorly understood, which hinders our ability to understand the effects of large-scale afforestation programs on soil nutrients and the capacity to sequester C.

In this study, we examined net N and C storage and C:N among soil pools in response to afforestation through our large-scale field sampling sites in northern China—a focus of afforestation during past decades (Bryan et al., 2018; Duan et al., 2011; He et al., 2015), and further evaluated for broader complementary effects vis-à-vis our study sites by mining the peer-reviewed scientific literature worldwide. With the world's largest area of planted forests (FAO, 2016; Piao et al., 2009; State Forestry Administration of the People's Republic of China, 2014), China has launched ambitious programs of afforestation that have contributed substantially to the sequestration of C (Hong et al., 2020; F. Lu et al., 2018; Shi & Han, 2014; Shi et al., 2013), thus it provides an ideal framework to investigate the effect of afforestation. A pairwise sampling method was conducted for the field campaign in northern China and only studies with the paired method were selected in the global metadata compilation. Compared with chronosequence and repeated sampling (D. Li et al., 2012; Shi & Han, 2014; Shi et al., 2013), paired sampling quantifies the opportunity costs of afforestation well (Hong et al., 2020; F. Lu et al., 2018) because it controls for the effects of other factors such as climate change and N deposition. Based on the comprehensive multiscale investigation of field-paired sampling data in the representative region (Figure 1a, $n = 610$) and the global meta data set of paired studies (Figure 1b, $n = 211$), we explored the impacts of afforestation on soil N and C:N and further investigated the major controlling factors of soil C and N dynamics after afforestation.

2. Materials and Methods

2.1. Study Design

In this study, afforestation includes both typical afforestation (i.e., planting trees in area with no forest history) and reforestation (planting trees in area with forest in last 50 years). We conducted a systematic field campaign from representative afforested areas in northern China and compiled a meta-data set at the global scale from 86 peer-reviewed papers. We surveyed 610 afforested plots and 161 control plots in northern China, which constituted 610 afforested-control pairs (some control plots were used more than once). We collected data from 211 study sites exploring changes in soil organic carbon (SOC) and soil total nitrogen (STN) caused by afforestation at the global scale from peer-reviewed papers, all of which also used pairwise sampling method.

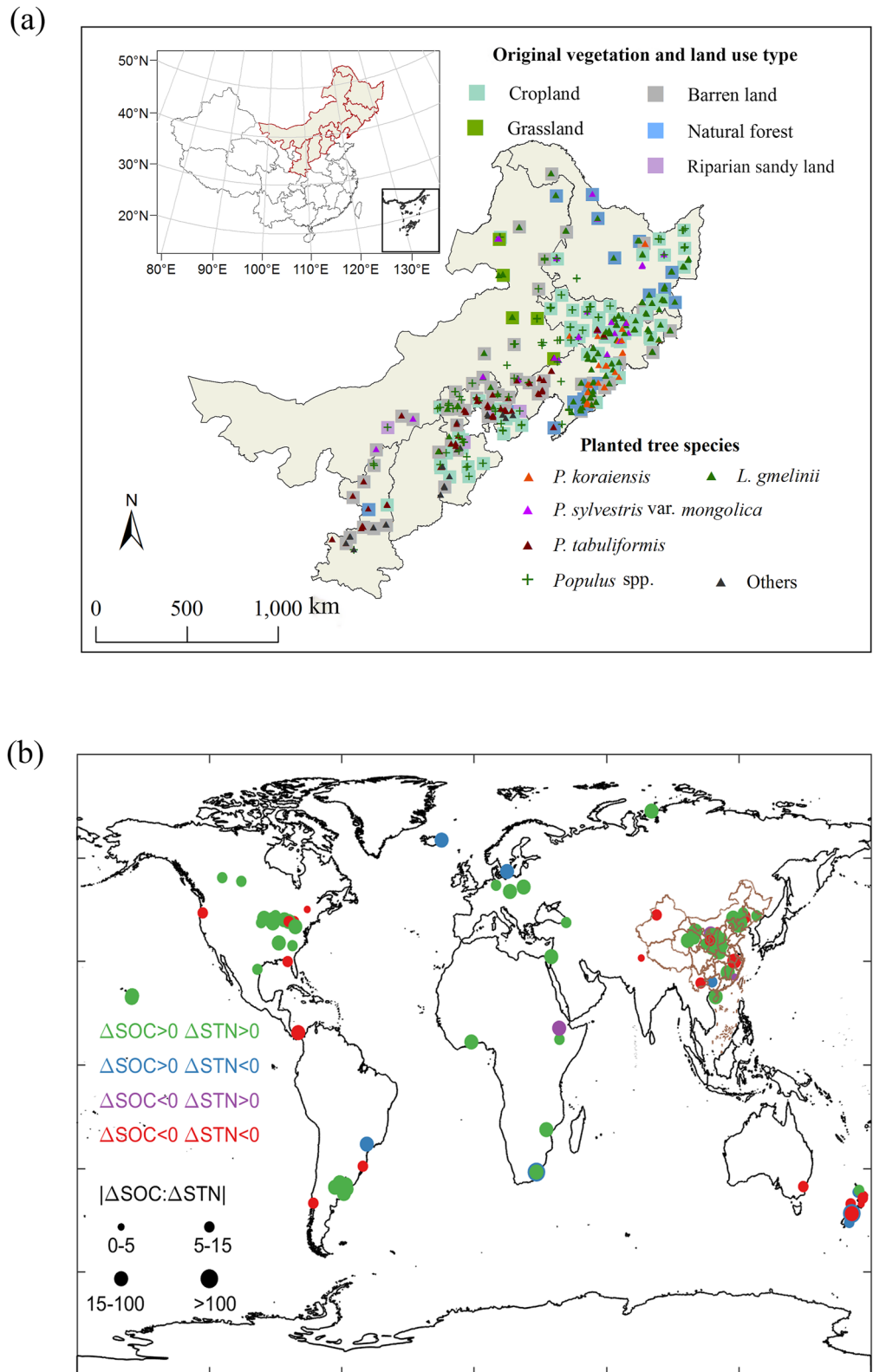


Figure 1. Distribution of the study sites. (a) Distribution of the sampling plots in northern China. The rectangles indicate the control plots, and colors indicate the original vegetation and land use type. Triangles and + indicate the plots afforested with different tree species. The inset shows the location of the study region in China. (b) Distribution of the global study sites collected from published papers. The color of each point indicates the type of change to soil organic carbon and soil total nitrogen, and the size represents the absolute value of $\Delta\text{SOC}:\Delta\text{STN}$.

2.2. Field Sampling Region

The field work was conducted in six provinces (Heilongjiang, Jilin, Liaoning, Hebei, Shanxi, and Shaanxi) and Inner Mongolia Autonomous Region in northern China (Figure 1a). This region extends from 34.20 to 51.80°N and 106.81 to 133.31°E, so the climate and soil vary greatly. Mean annual temperature (MAT) ranges from -3°C to 15°C , and mean annual precipitation (MAP) ranges from 355 to 1,068 mm. This region contains multiple soil types, including black soil, bog soil, brown coniferous forest soil, brown earths, brown pedocals, castanozems, chernozems, cold brown calcic soil, yellow earths, and yellow-brown earths (Xiong & Li, 1987), approximately corresponding to phaeozems, gleysols, humic cambisols, haplic/albic luvisols or eutric/dystric cambisols, haplic calcisols, kastanozems, chernozems, cambisols, haplic alisols, and ferric/haplic luvisols, respectively, in the soil classification of the United Nations Food and Agriculture Organization (Xie et al., 2007).

This region is a focus of afforestation in China (Piao et al., 2009; State Forestry Administration of the People's Republic of China, 2014) with more than 120,000 km² of planted forest, most of which was due to the Three North Shelterbelt Development Program (He et al., 2015).

2.3. Field Sampling Methods

Pairwise sampling was used to determine the impact of afforestation on STN and SOC in the field studies. We chose one nonafforested plot in the planted area at each site as the control plot to represent the soil properties without afforestation. Several afforested plots (1–26) with different planted tree species or stand ages were selected around the control plot. The vegetation and land use type of the control plot could represent the land-use history in the afforested plot before afforestation. The distance between any afforested plot and its corresponding nonafforested-control plot was usually 50–100 m to minimize the variation in soil and climatic properties between the pair and the largest acceptable distance was not more than 2.5 km in very few plots. The original vegetation and land use types (OVLUT) included cropland, barren land, grassland, natural forest, and riparian sandy land. Note that natural forest control plots indicate their corresponding afforested plots used to be natural forests that have been clear-cut and then reforested during the afforestation campaign. Each afforested plot and its corresponding control plot therefore constituted an afforested-control pair, with the difference between them representing the impact of afforestation. We examined 610 afforested plots and 161 control plots, representing 610 afforested-control pairs. All afforested plots were monocultures, so we could easily document the tree species. The main tree species were *Pinus koraiensis*, *Pinus sylvestris* var. *mongholica*, *Pinus tabulaeformis*, *Larix gmelinii*, and *Populus* spp. (including *Populus simonii*, *Populus* × *beijingensis* and *Populus* × *xiaohei*) and some minority species, which were marked as others. In each plot, we dug three replicate soil profiles in the diagonal direction and collected samples from different layers (0–5, 5–10, 10–20, 20–30, 30–60, and 60–100 cm) using a cutting ring of 100 cm³. We collected 18 samples in each plot except for a few plots where we could not reach a depth of 1 m. In total, we selected a total of 11,610 samples for the study. Note that we collected two identical cutting rings of soils at each depth, one of which would later be oven-dried while the other air-dried. We measured the height and diameter at breast height of each tree in the afforested plots for calculating biomass using allometric equations (Fang et al., 1996). Additional data such as the year of afforestation (stand age) were obtained from local forestry administrations.

2.4. Laboratory Methods

All soil samples were brought back to the laboratory and then air dried. Stones and roots were removed from air-dried samples by passing through 2-mm sieves. We oven-dried soils (one cutting ring) and got the soil dry weight (SDW). The remaining sieved soils (the other cutting ring) were prepared for chemical analyses. Soil pH was measured in 1:2.5 mixtures of soil and deionized water using a pH meter (PHS-3C, Lei-ci, China). Soil solutions were shaken for 30 min and then kept static for 5 min before pH measurement. The soil inorganic C concentration (SICC) was measured using a 08.53 CALCIMETER (M1.08.53.E, Eijkelkamp, Netherlands). SICC in our study was equivalent to the carbonate concentration in carbon dioxide (CO₂) emissions digested using strong acid (0.2 mol L⁻¹ HCl). Soil total N concentration (STNC) and soil total C concentration (STCC) were measured using an elemental analyzer (Viro el cube, Elementar, Germany) after the samples were subsequently passed through 1-mm sieves.

2.5. Metadata Compilation

We collected data from published papers using the Web of Science to investigate the dynamics of SOC and STN after afforestation on a global scale. The following criteria were used to select the papers: SOC density and STN density were both reported or could be calculated using SOC and STN concentrations, soil bulk density, and sampling depth; pairwise sampling was used for obtaining data for both the afforested and control (nonafforested) sites and data for mineral soil were included. This data set included a total of 211 sites reported in 86 peer-reviewed papers. We extracted planted tree species in each site from the papers, and then obtained the corresponding symbiotic mycorrhizal type for each tree species according to data provided by Wang and Qiu (2006) and Soudzilovskaia et al. (2020). The distribution of the mycorrhiza types associated with planted trees is shown in Figure S1 in Supporting Information S1, which was mainly driven by temperature and precipitation.

2.6. Other Data

MAP and MAT were obtained from the China Meteorological Forcing Data set, which was created by merging a variety of data sources (Chen et al., 2011; Yang et al., 2010), with a spatial resolution of $0.1 \times 0.1^\circ$ and a temporal resolution of 3 hours. Data for net primary productivity (NPP) were obtained from the Moderate Resolution Imaging Spectroradiometer MOD17A3 data set (Running, 2015). Data for soil type and clay concentration were obtained from the Harmonized World Soil Database v.1.2 (FAO et al., 2012). We also obtained data for N deposition from the Multi-Scale Synthesis and Terrestrial Model Intercomparison Project Nitrogen Deposition Enhanced Dentener data set (Wei et al., 2014), which includes ammonium N (NH_x) deposition and nitrate N (NO_x) deposition at a resolution of $0.5 \times 0.5^\circ$ for 1860–2050. Means of the 10-year data before field sampling (2003–2012) were used in the data analysis. To obtain the global potential afforestation area, global potential tree cover data (Bastin et al., 2019) (pixels with tree cover >20% were defined as potential forest), existing tree cover data (Hansen et al., 2013) (pixels with tree cover >20% were defined as existing forest), and data for agricultural and urban areas (Arino et al., 2012) were used. We used global potential forest pixels removing existing forest pixels, agricultural, and urban pixels to get the potential afforestation pixels. Data for global STN were obtained from world soil property estimates for broadscale modeling (WISE30sec) (Batjes, 2015).

2.7. Data Analysis

Soil organic C concentration (SOCC) was calculated using STCC and SICC:

$$\text{SOCC} = \text{STCC} - \text{SICC} \quad (1)$$

Soil total nitrogen density (STN_j) and SOC density (SOC_j) in each soil layer (j indicates the j th layer, e.g., $j = 1$ indicate the first layer (0–5 cm) while $j = 6$ indicates the sixth layer (60–100 cm)) was calculated using STNC_j and SOCC_j , SDW (SDW_j), the volume of cutting ring (V), and the thickness of the layer (w_j):

$$\text{STN}_j = \text{STNC}_j * \frac{\text{SDW}_j}{V} * w_j * 10^2 \quad (2)$$

$$\text{SOC}_j = \text{SOCC}_j * \frac{\text{SDW}_j}{V} * w_j * 10^2 \quad (3)$$

Each plot had three replicate profiles, so mean STN_j and SOC_j for the three profiles were used in the analysis. The sum of mean STN_j and SOC_j in all layers was used to represent STN and SOC in each plot:

$$\text{STN} = \sum_{j=1}^6 \text{STN}_j \quad (4)$$

$$\text{SOC} = \sum_{j=1}^6 \text{SOC}_j \quad (5)$$

We defined ΔSTN and ΔSOC due to afforestation as the differences of STN and SOC between the afforested and control plots (Equations 6 and 7) at both the plot and layer levels. Note that STN and SOC were corrected to equivalent soil masses because afforestation can also affect soil density:

$$\Delta\text{STN} = \text{STN}(\text{afforested}) - \text{STN}(\text{control}) \quad (6)$$

$$\Delta\text{SOC} = \text{SOC}(\text{afforested}) - \text{SOC}(\text{control}) \quad (7)$$

We also calculated mean layer differences in SOC and STN using ΔSOC and ΔSTN in each layer divided by the corresponding layer thickness, respectively, to make the result comparable in the vertical direction.

The C:N ratio was calculated using Equation 8 for both the plot and layer levels, and $\Delta(\text{C:N})$ was then calculated using Equation 9:

$$\text{C} : \text{N} = \text{SOC} : \text{STN} \quad (8)$$

$$\Delta(\text{C} : \text{N}) = \text{C} : \text{N}(\text{afforested}) - \text{C} : \text{N}(\text{control}) \quad (9)$$

ΔSTN , ΔSOC , and $\Delta(\text{C:N})$ for the set of metadata were also calculated using Equations 6–9. For the metadata, STN and SOC were calculated based on Equations 2 and 3 if they were not directly reported. Differences in C:N were calculated using Equations 8 and 9.

Paired Student's *t*-tests were used to compare soil properties (STN, SOC, C:N) in the control and afforested groups for both the sampling data set and the set of metadata. Independent sample *t*-tests were used to determine whether the differences due to afforestation differed significantly from 0. False discovery rates were corrected to control potential error rates in multiple comparisons (Benjamini & Yekutieli, 2001). Ordinary least squared regression was performed to determine the relationships between variables. We estimated the uncertainties of the regression between ΔSTN and STN in control groups (STN_c) using bootstrapping, where we randomly selected 80% of the samples in each group to run the regression and repeated the random selection and regression for 1,000 times. We also conducted an analysis of covariance (ANCOVA) to explore whether regression slopes between ΔSTN and ΔSOC were significantly different among tree species groups. Moreover, given that previous studies indicated that many factors such as climate, soil type, OVLUT could regulate afforestation-induced changes in soil C and N (Berthrong et al., 2009; D. Li et al., 2012), we constructed boosted regression trees (BRTs) (Elith et al., 2008; Friedman, 2002; Friedman & Meulman, 2010) to evaluate the effects of all factors (MAP, MAT, NPP, soil type, tree species, OVLUT, stand age, clay concentration, SOC in the control groups, STN_c, pH in the control groups, N deposition, and C:N in the control groups) on ΔSTN (Figure S2 in Supporting Information S1). The BRT model well identified the variation of ΔSTN , which we then used to calculate the relative importance of each factor (Friedman, 2002; Friedman & Meulman, 2010).

Finally, we used error-based simulation to evaluate the robustness of the results accounting for the colinearity between ΔSTN and STN_c (Hong et al., 2020) (Figure S3 in Supporting Information S1) because the negative correlation between ΔSTN and STN_c may have been confounded by observed errors. For each simulation, the “starting” STN_c was the observed value. The “starting” STN_f was calculated as the starting STN_c plus a random change (drawn from a distribution with the same mean and standard deviation as the observed ΔSTN). The starting ΔSTN and STN_c were thus not correlated. We then added a random error to the starting STN_c to create a “final” STN_c and a separate uncorrelated error to the starting STN_f to create the “final” STN_f. We then calculated the “final” ΔSTN as final STN_f—final STN_c. The final ΔSTN contained the error added to STN_c, so we expected a negative correlation between final ΔSTN and final STN_c. We conducted a regression analysis between final ΔSTN and final STN_c to obtain the slope and *P* value of this “null” negative correlation. The slope gradually decreased as the proportional error increased (from 0.01 to 1), and the *P* value also decreased. This process was repeated 100 times for each increase in proportional error to obtain a mean. The results are shown in Figure S3 in Supporting Information S1. For the sampling data (Figure S3a in Supporting Information S1), the required proportional error needed to be >0.35 to obtain the observed slope from this “null” relationship, which was much higher than the observed mean error of 0.18. For the observed mean proportional error of 0.18, the “null” slope was -0.11 and 0 time in 100 times could produce an observed slope of -0.37 , indicating that the observed negative correlation between ΔSTN and STN_c was robust for the sampling data. The same methods were used for the combined data, where the results indicated that the negative correlation

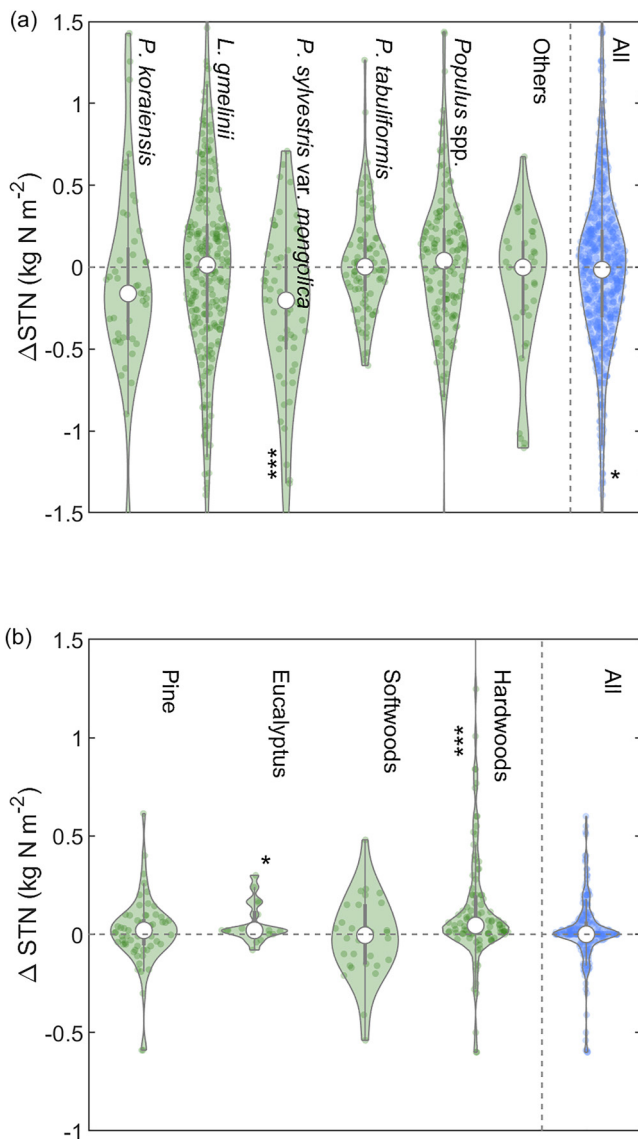


Figure 2. Comparison of Δ STN across tree species. (a) Δ STN for the sampling data. (b) Δ STN for the metadata. The whiskers indicate the distributions of the samples, and the white circles indicate the medians. *, **, and *** indicate that the null hypothesis can be rejected at $P < 0.05$, 0.01 , and 0.001 , respectively, in independent sample t -tests with correction of false discovery rates.

between Δ STN and STN_c was also robust (Figure S3b in Supporting Information S1). Testing the metadata results was not necessary because they were not significant.

3. Results

3.1. Changes in Soil N With Afforestation

The responses of STN to afforestation varied among planted tree species at both regional and global scales (Figure 2). STN with afforestation in the intensively sampled sites in northern China was significantly lower by 0.05 kg N m^{-2} at depths of 0–1 m after correcting for the equivalent soil mass (Figure 2a, $P < 0.05$), mostly driven by *P. sylvestris* var. *mongolica*. Non-significant difference was observed between STN in control and afforested groups in the global data set based on the synthesis of previous studies (Figure 2b), with the most pronounced response for soils planted with hardwoods ($P < 0.001$), including eucalyptus ($P < 0.05$). Pine and other softwoods did not significantly affect STN. The change in STN also varied across sampling depth and stand age (Figure S4 in Supporting Information S1). Δ STN varied greatly with depth in young forests (0–10 years). STN with afforestation generally increased in the topsoil (0–5 cm) but decreased in soil below 5 cm in older forests (>20 years).

Based on the results of BRT (Figure S2 in Supporting Information S1), STN_c had the highest importance in regulating soil N dynamics after afforestation. Therefore, we explored the relationship between Δ STN and STN_c to further investigate the divergent responses of STN to afforestation at regional and global scales (Figure 3). Δ STN and STN_c were negatively correlated (Figure 3a, $P < 0.001$), indicating that afforestation increased STN in STN-poor soils but decreased it in STN-rich soils. This correlation was mainly driven by sampling data from northern China ($P < 0.001$), and the relationship in the global meta-analysis was only marginally significant ($P = 0.08$). The simulation demonstrated the robustness of the negative correlation between Δ STN and STN_c for the sampling and combined data (Figure S3 in Supporting Information S1), where the error-based slope was not able to attain the level of the observed slope. Thus, we further divided the data based on STN in the control groups (Figure 3b). Soil total nitrogen significantly increased with afforestation in the group with STN_c $< 1 \text{ kg N m}^{-2}$ (depths of 0–1 m), accompanied by increased SOC. In contrast, both STN and SOC significantly decreased in the groups with STN_c $> 2 \text{ kg N m}^{-2}$ (depths of 0–1 m). STN with afforestation significantly decreased in the group with STN_c between 1 and 2 kg N m^{-2} (depths of 0–1 m) with nonsignificant effects on SOC. The dependence of Δ STN and Δ SOC on STN_c was generally observed in groups with different OVLUT (Figure S5 in Supporting Information S1) and stand age (Figure S6 in Supporting Information S1), indicating that these two factors did not confound the dominant role of STN_c in regulating postafforestation soil C and N dynamics.

We defined the threshold STN (T_n), that is, the inflection point where Δ STN changes from positive to negative, as the horizontal axis intercept of the ordinary least squared regression line in Figure 3a. The estimated T_n was at 0.86 (95% CI: 0.81 – 0.91) kg N m^{-2} at depths of 0–1 m using a bootstrapping method (see Section 2), which divided the sampled soils into low (< 0.86) and high ($> 0.86 \text{ kg N m}^{-2}$) N groups. We further investigated the divergent dynamics of STN with stand age in the two groups (Figure S7 in Supporting Information S1). Afforestation increased STN in the low-N group at all age groups, and this impact was significant at stand ages of 10–20 and 30–40 years (Figure S7a in Supporting Information S1). In contrast, afforestation significantly decreased STN

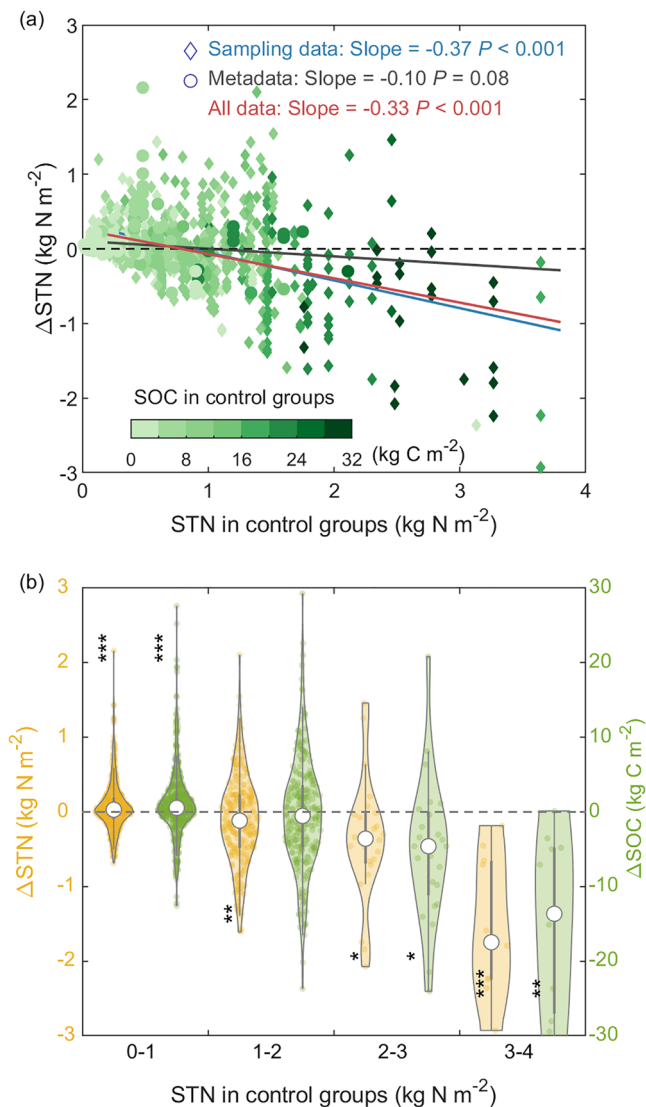


Figure 3. Control of initial soil total nitrogen (STN) on soil C and N dynamics after afforestation. (a) Relationships between Δ STN and control STN from the sampling data, metadata, and all data. Ordinary least squared regressions were conducted between Δ STN and control STN using the means of the slopes and intercepts with 100 bootstrapping iterations (see Section 2). The color scale indicates the amount of soil organic carbon in the control groups. (b) Comparisons of Δ STN and Δ SOC across groups with different control STNs. The whiskers indicate the distribution of the samples, and the white circles indicate the medians. Independent sample *t*-tests with correction for false discovery rates were conducted to compare the data of each group with 0. *, **, and *** indicate that the null hypothesis can be rejected at $P < 0.05$, 0.01, and 0.001, respectively.

in the high-N group at stand ages of 10–40 years, but not significantly in the group with stand age >40 years (Figure S7b in Supporting Information S1).

3.2. Change of Soil C and N Interactions After Afforestation

The responses of soil N to afforestation differed at regional and global scales, but soil N and C were strongly coupled across data sets (Figure 4). The relationships between Δ SOC and Δ STN yielded a slope of 9.69 for all sampling data combined. Interestingly, the regression slopes between Δ SOC and Δ STN showed significant differences among species ($P < 0.001$ for ANCOVA, Figure 4a), which suggests a divergent C change accompanied with per unit N change induced by afforestation with different tree species. Specifically, the slope was largest for *L. gmelinii* (11.60), indicating the highest rates of C gain/loss per unit change in N. In contrast, *Populus* spp. had the smallest changes in C per unit change in N (slope = 5.85). The slopes for *P. koraiensis*, *P. sylvestris* var. *mongholica*, *P. tabuliformis*, and others were 9.87, 10.41, 9.42, and 7.50, respectively. The metadata provided similar results, where per unit change in N was accompanied by 11.68 units of C change with afforestation (Figure 4b). The slope was largest for eucalyptus (14.96) and smallest for pine (9.53). The slopes for hardwoods (excluding eucalyptus) and softwoods (excluding pine) were 12.10 and 11.88, respectively. However, it is noteworthy that the difference in slopes among species groups was nonsignificant ($P = 0.33$ for ANCOVA), which may be because hardwood and softwood included multiple tree species.

We explored the changes in SOC and STN and their relationships at different depths to determine whether the dynamics of SOC and STN varied vertically (Figure S8 in Supporting Information S1). Both C and N in the topsoil (0–5 cm) increased with afforestation, but both C and N decreased below 5 cm (Table S1). The dynamics between STN and SOC were also coupled at different depths, where the slopes varied between 7.10 and 10.76 but did not show a vertical trend (Figure S8 in Supporting Information S1).

With afforestation, C:N was higher than control groups for both the sampling data and the global metadata (Figure S9 in Supporting Information S1). For the sampling data, C:N significantly increased only for *L. gmelinii*, with nonsignificant changes in C:N in the other groups. The higher C:N with afforestation was majorly contributed by sites with high initial soil N (Figure S7 in Supporting Information S1), especially for the plantations older than 20 years. The change in C:N for the low-N group was not significant and varied greatly. For the global metadata, C:N significantly increased for Eucalyptus, softwoods including pine, but nonsignificant difference was observed in the group of hardwoods excluding Eucalyptus. Interestingly, C:N only significantly increased where ectomycorrhizal trees were planted, although STN was higher for all mycorrhizal types (Figure S10 in Supporting Information S1).

The relative abundance of C and N (C:N) in background soil also regulated the changes in C:N (Figure 5a). C:N with afforestation tended to decrease in soil with relatively higher initial C:N but increased in soil with lower initial C:N. An age threshold was also observed for different depths (Figure 5b). The changes in soil C:N with afforestation were not significant at any depth when stand age was <30 years. C:N generally increased in the group of 30–40 years, which showed significant changes at depths of 0–5 and 20–30 cm. C:N with afforestation significantly increased at depths of 60–100 cm for stand age >40 years.

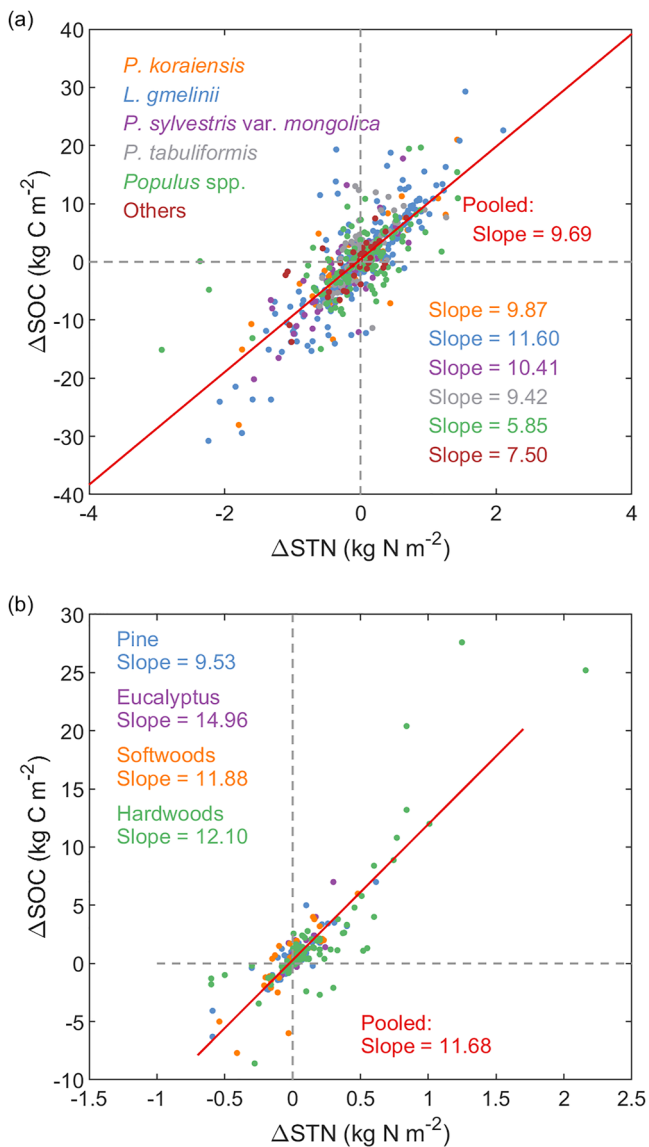


Figure 4. Dynamics of soil total nitrogen and soil organic carbon. (a) Relationship between Δ SOC and Δ STN across six tree species and all species pooled in the sampling data. (b) Relationship between Δ SOC and Δ STN across the study sites collected from the published papers. The red lines are the ordinary least squared regression lines.

Collectively, the dynamics of both soil C and N after afforestation were regulated by background soil N status. At the global scale, soil N is lower than T_n (0.86 kg N m⁻² in 0–1 m depth) in 45% of the potential afforestation area, which indicates a potential soil C sink with afforestation. In contrast, in the remaining 55% area, soil N is higher than T_n , indicating a risk of soil C and N loss after afforestation (Figure 6).

4. Discussion

This study provides a comprehensive understanding on the dynamics of N and C–N interactions with afforestation in both intensively sampled northern China and extensively synthesized global sites. We found initial soil N stock was the dominant factor controlling Δ STN, with much higher importance than the other factors, such as tree species, precipitation, temperature, soil type, OVLUT etc. Both STN and SOC increased with afforestation in areas with low initial STN, but decreased in areas with high initial STN. The coupled dynamic of C and N depending on initial soil N status implies that the N cycle driven by plant physiological activity may regulate the dynamics of soil organic matter (SOM) (Mooshammer et al., 2014).

The N sources of ecosystem generally include atmospheric N deposition, biological fixation, and rock weathering (Houlton et al., 2018; Morford et al., 2016), while N output includes gaseous and aqueous export (Mason et al., 2022). There is no evidence that afforestation widely affects biological N fixation, but it can impact other N sources and output to regulate ecosystem N balance (Gundersen et al., 2006; Heil et al., 2007; Henneron et al., 2020). First, afforestation increases the surface roughness and collecting surface area (Gundersen et al., 2006; Heil et al., 2007). The forest canopy can directly absorb the deposited N and transfer the absorbed N to roots or input to soil as litter (Nair et al., 2016; Wang et al., 2021). Second, planted trees generally have a deeper root system than original vegetation, so that they can absorb more N from deep soils and groundwater, and thus reduce gaseous and aqueous N losses from the ecosystem (Brady & Weil, 2008; Hobbie, 2015). Third, afforestation could reduce nitrate leaching by substantially increasing evapotranspiration, regardless of the species of planted trees (Y. Li et al., 2018). These processes indicate the increase (increasing input and decreasing output) of soil N induced by afforestation. However, afforestation can also intensify N mineralization through a strong priming effect, and thus increase the gaseous and aqueous N losses (Henneron et al., 2019, 2020). Given that most soil N is stored in SOM (Brady & Weil, 2008), the changes in SOC and STN are strongly coupled (see Figures 3 and 4).

In areas with low soil N stock, the increased N can be efficiently used by planted trees (X. Lu et al., 2021) and litters further recharge SOM. At the same time, the loss of soil C and N induced by the priming effect is low due to the limited amount of initial SOM. Therefore, both SOC and STN increase after afforestation in low-N areas, especially for the topsoil (Table S1). In contrast, in areas with high initial STN, soils can provide more nutrients through decomposition and mineralization and support higher plant biomass than SOM-poor soils (Figure S11 in Supporting Information S1). Higher plant biomass leads to a stronger priming effect and thus stimulates N mineralization via SOM decomposition (Brady & Weil, 2008; Schimel & Bennett, 2004), which leads to a positive feedback between plant growth and SOM decomposition (Brady & Weil, 2008). Litters recharge the SOM pool but cannot fully offset the decomposition loss so that both STN and SOC decrease after afforestation. Topsoil receives the largest litter input (Brady & Weil, 2008), resulting in the least decrease in STN and a nonsignificant increase in SOC (Table S1).

Plant uptake and microbial decomposers also regulate changes in C:N in soils with different C and N concentrations (Henneron et al., 2020; Mooshammer et al., 2014). In N-rich soils, plant uptake of N and litter input

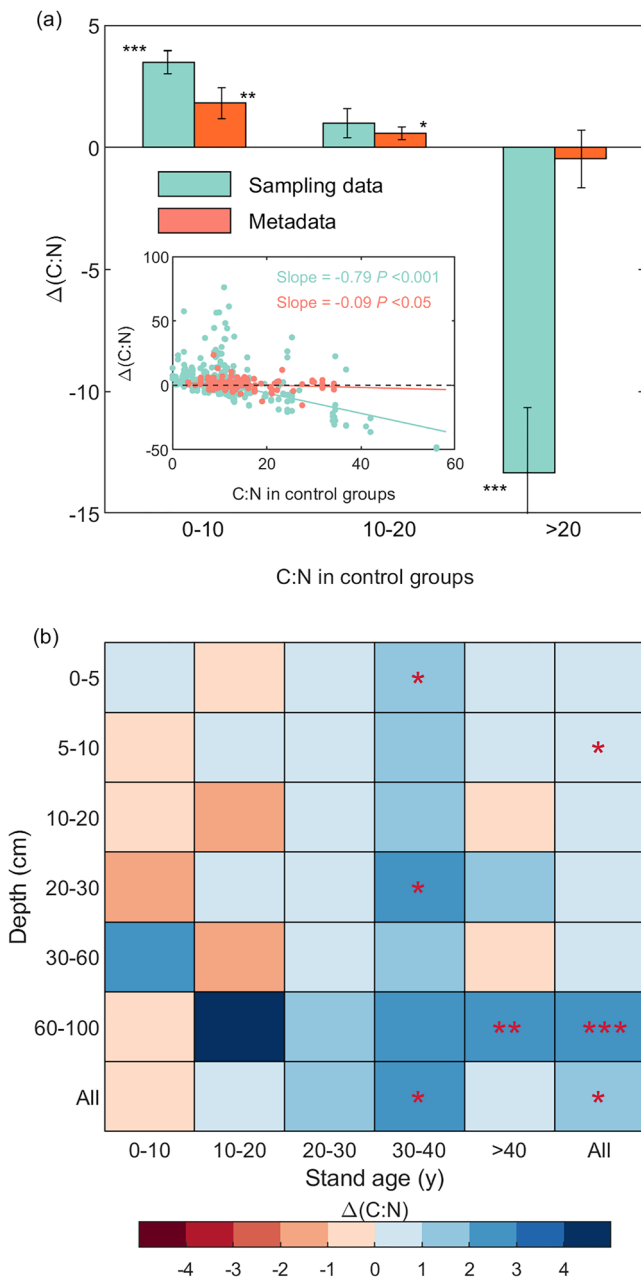


Figure 5. Changes in C:N ($\Delta(C:N)$) induced by afforestation. (a) Comparison of $\Delta(C:N)$ in groups with different background C:N. The inset shows the relationships between $\Delta(C:N)$ and control C:N from the sampling data and metadata. (b) Vertical comparisons of $\Delta(C:N)$ in the various age groups. This result is based only on the sampling data because the metadata is insufficient to conduct a vertical comparison. Independent sample *t*-tests with correction for false discovery rates were conducted to compare the data of each group with 0. *, **, and *** indicate that the null hypothesis can be rejected at $P < 0.05$, 0.01, and 0.001, respectively.

(higher C:N comparing with soil) increase C:N, which becomes larger with age (Figure S7b in Supporting Information S1). In N-poor soils, although both soil C and N increased with afforestation, we did not find a significant increase in C:N after afforestation (Figure S7a in Supporting Information S1), which may be due to the increase in inorganic N input through deposited N capture after afforestation (Henneron et al., 2019, 2020). Microbes can also adjust their C and N use efficiencies depending on the C:N stoichiometry of SOM (Janssen, 1996; Mooshammer et al., 2014). Specifically, microbes retain high efficiencies of N use when N is more limited than C (high soil C:N) and thus reduce potential N losses by providing fewer substrates for nitrification and consequent losses through gaseous N forms. In contrast, when C is more limited than N (low soil C:N), the microbial N use efficiencies are low, resulting in higher N mineralization and gaseous N losses (Mooshammer et al., 2014). This adjustment of microbial nitrogen use efficiency to C-N imbalances leads to divergent changes of C:N caused by afforestation in soils with different relative abundances of C and N. Interestingly, the increase in C:N for the metadata was notably driven mostly by trees with ectomycorrhizal associations. This indicates a higher N use efficiency and afforestation with ectomycorrhizal trees may therefore store more C per unit N in soil than afforestation with arbuscular mycorrhizal trees.

Afforestation may also directly and indirectly affect the soil N cycle via other mechanisms. For instance, afforestation can affect the emission and leaching of nitrous oxide by affecting soil pH (Hénault et al., 2019), although the overall direction and magnitude of this effect remain uncertain. Moreover, both free-living and symbiotic N fixation rates tend to increase in response to increased carbon availability (Houlton et al., 2008; Reed et al., 2011; Vitousek et al., 2002), which could be especially important in N-poor sites; but can also be triggered via long-term feedback in N-rich environments that are underlain by N-rich parent materials (Dynarski et al., 2019). The extent to which plant-soil-microbe feedback triggered an increase in free-living biological N fixation with afforestation offers a compelling area for future mechanistic inquiry.

The field sampling data well characterized the effect of STN_c on changes to STN, but the relationship in the global metadata was weak and unreliable, for two possible reasons, including a lack of spatial coverage of studies and variation across soil depths. Most (95%) of the metadata sites were in regions with relatively low STN ($< 1 \text{ kg N m}^{-2}$), so STN change was nonsignificant. Thus, a well-designed global-scale sampling study with different background soils is needed. Further, afforestation usually increases STN in topsoil but decreases it in deep soils. Our sampling depth in northern China was 1 m, but the sampling depths for the metadata studies were usually $< 1 \text{ m}$. Changes in STN for the metadata results were weak due to insufficient sampling depth and the absence of a negative correlation between ΔSTN and STN_c . Both intensive and extensive sampling studies are therefore essential for determining soil C and N storage after afforestation.

Our results indicated that the dynamics of soil C and N after afforestation were coupled for all depths, which were context-dependent. Afforestation increased STN in low-STN areas and thus increased soil C, and afforestation slightly decreased STN in high-STN areas, leading to the loss of soil C. Therefore, the potential of the soil C sink was regulated by the status of soil N. A recent study by Bastin et al. (2019) suggested that tree restoration has the potential to sequester as much as 205 Gt C in ecosystems. Our result, however, indicated the risk of soil C loss at more than half of the potential afforestation area (Figure 6), given that afforestation could stimulate SOC decomposition in regions with higher background soil N stock.

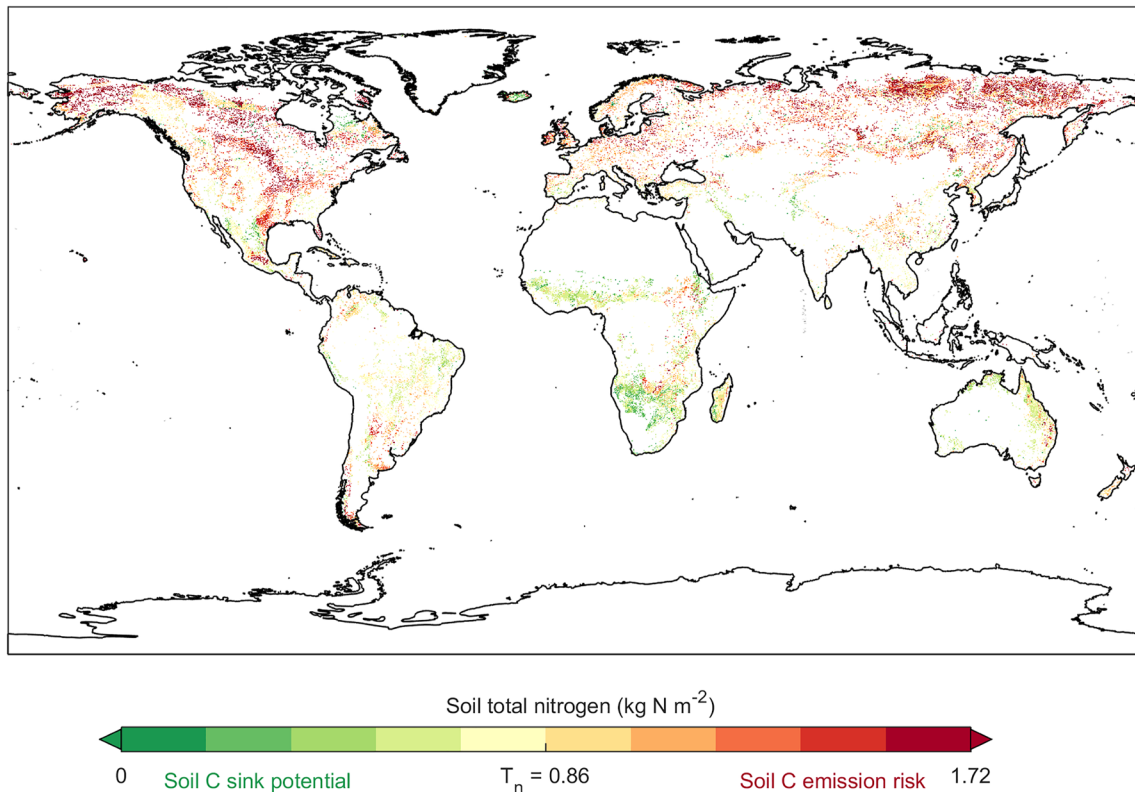


Figure 6. Soil total nitrogen (STN) in global potential afforestation area. T_n indicates the threshold of STN in Figure 3a. Global potential afforestation area is using global potential tree cover (Bastin et al., 2019) to remove existing tree cover (Hansen et al., 2013) and agricultural and urban areas (Arino et al., 2012). For the data of global potential tree cover and existing tree cover, only data with tree cover >20% was used.

Hence, the estimated afforestation C sink potentials that do not account for the background soil N threshold may be overly optimistic (Bastin et al., 2019). Moreover, even assuming that this potential is accurate and achievable, based on the coupled dynamics of C and N in our study, a large amount of extra N would be required. The demand for N remains very high even considering the spatial heterogeneity and higher C:N in biomass than soil (Peñuelas et al., 2019). Increasing the N-use efficiency of an ecosystem is therefore important for enhancing the C-sink potential. The different change ratios of C and N (i.e., the change of C per change of N) among tree species may have been due to the different stoichiometric ratio of tree species (Peñuelas et al., 2019; Sardans et al., 2021), suggesting that the choice of tree species also affects the N-use efficiency. Although afforestation may decrease soil C in N-rich soils, the C loss would be offset by the increase in biomass C (Fang et al., 2001). Afforestation therefore has the potential to increase the C sink, but choosing appropriate species and strategies of nutrient management based on background environmental conditions are still important for maximizing the sequestration of C.

Conflict of Interest

The authors declare no conflicts of interest relevant to this study.

Data Availability Statement

The field data related to this research are available at figshare (<https://doi.org/10.6084/m9.figshare.21341577>).

Acknowledgments

This work was supported by the National Key R&D Program of China (2019YFA0607304) and the Explorer Prize. S.B. Hong acknowledges the support from the Postdoctoral Innovation Talents Support Program of China (Grant BX2021005).

References

- Arino, O., Perez, J., Kalogirou, V., Bontemps, S., Defourny, P., & Bogaert, E. (2012). *Global land cover map for 2009 (GlobCover 2009)*. European Space Agency, Université catholique de Louvain, PANGAEA. <https://doi.org/10.1594/PANGAEA.787668>
- Bastin, J. F., Finegold, Y., Garcia, C., Mollicone, D., Rezende, M., Routh, D., et al. (2019). The global tree restoration potential. *Science*, 365(6448), 76–79. <https://doi.org/10.1126/science.aax0848>
- Batjes, N. (2015). World soil property estimates for broad-scale modelling (WISE30sec, v.1.0) Report 2015/01 (ISRIC Soil Data Hub).
- Benjamini, Y., & Yekutieli, D. (2001). The control of false discovery rate in multiple testing under dependency. *Annals of Statistics*, 4, 1165–1188. <https://doi.org/10.1214/aos/1013699998>
- Berthrong, S. T., Jobbágy, E. G., & Jackson, R. B. (2009). A global meta-analysis of soil exchangeable cations, pH, carbon, and nitrogen with afforestation. *Ecological Applications*, 19(8), 2228–2241. <https://doi.org/10.1890/08-1730.1>
- Brady, N., & Weil, R. (2008). *The nature and properties of soils*. Prentice-Hall Press.
- Bryan, B., Gao, L., Ye, Y., Sun, X., Hou, X., Crossman, N. D., et al. (2018). China's response to a national land-system sustainability emergency. *Nature*, 559(7713), 193–204. <https://doi.org/10.1038/s41586-018-0280-2>
- Chen, Y., Yang, K., He, J., Qin, J., Shi, J., Du, J., & He, Q. (2011). Improving land surface temperature modeling for dry land of China. *Journal of Geophysical Research*, 116(D20), 999–1010. <https://doi.org/10.1029/2011JD015921>
- Cotrufo, M. F., Ranalii, M. G., Haddix, M. L., Six, J., & Lugato, E. (2019). Soil carbon storage informed by particulate and mineral-associated organic matter. *Nature Geoscience*, 12(12), 989–994. <https://doi.org/10.1038/s41561-019-0484-6>
- Duan, H. C., Yan, C. Z., Tsunekawa, A., Song, X., Li, S., & Xie, J. L. (2011). Assessing vegetation dynamics in the Tree-North Shelter Forest region of China using AVHRR NDVI data. *Environmental Earth Sciences*, 64(4), 1011–1020. <https://doi.org/10.1007/s12665-011-0919-x>
- Dynarski, K. A., Morford, S. L., Mitchell, S. A., & Houlton, B. Z. (2019). Bedrock nitrogen weathering stimulates biological nitrogen fixation. *Ecology*, 100(8), e02741. <https://doi.org/10.1002/ecy.2741>
- Elith, J., Leathwick, J., & Hastie, T. (2008). Working guide to boosted regression trees. *Journal of Animal Ecology*, 77(4), 802–813. <https://doi.org/10.1111/j.1365-2656.2008.01390.x>
- Fang, J., Chen, A., Peng, C., Zhao, S., & Ci, L. (2001). Changes in forest biomass carbon storage in China between 1949 and 1998. *Science*, 292(5525), 2320–2322. <https://doi.org/10.1126/science.1058629>
- Fang, J., Liu, G., & Xu, S. (1996). Biomass and net production of forest vegetation in China. *Acta Ecologica Sinica*, 16, 497–508.
- FAO. (2016). *Global forest resources assessment 2015*. Food and Agricultural Organization of the United Nations.
- FAO, IIASA, ISRIC, ISSCAS, & JRC. (2012). *Harmonized world soil database (version 1.2)*. FAO and IIASA.
- Farley, K., Kelly, E., & Hofstede, R. (2004). Soil organic carbon and water retention following conversion of grasslands to pine plantations in the Ecuadorian Andes. *Ecosystems*, 7, 729–739. <https://doi.org/10.1007/s10021-004-0047-5>
- Friedman, J. (2002). Stochastic gradient boosting. *Computational Statistics & Data Analysis*, 38(4), 367–378. [https://doi.org/10.1016/S0167-9473\(01\)00065-2](https://doi.org/10.1016/S0167-9473(01)00065-2)
- Friedman, J., & Meulman, J. (2010). Multiple additive regression trees with application in epidemiology. *Statistics in Medicine*, 22(9), 1365–1381. <https://doi.org/10.1002/sim.1501>
- Gundersen, P., Schmidt, I., & Raulund-Rasmussen, K. (2006). Leaching of nitrate from temperate forests - Effects of air pollution and forest management. *Environmental Reviews*, 14(1), 1–57. <https://doi.org/10.1139/a05-015>
- Hansen, M. C., Potapov, P. V., Moore, R., Hancher, M., Turubanova, S. A., Tyukavina, A., et al. (2013). High-resolution global maps of 21st-century forest cover change. *Science*, 342(6160), 850–853. <https://doi.org/10.1126/science.1244693>
- He, B., Chen, A., Wang, H., & Wang, Q. (2015). Dynamic response of satellite-derived vegetation growth to climate change in the Three North Shelter Forest Region in China. *Remote Sensing*, 7(8), 9998–10016. <https://doi.org/10.3390/rs70809998>
- Heil, G. W., Muys, B., & Hansen, K. (2007). *Environmental effects of afforestation in North-Western Europe. From field observations to decision support*. Springer.
- Hénault, C., Bourennane, H., Ayzac, A., Ratié, C., Gall, C. L., Cohan, J. P., et al. (2019). Management of soil pH promotes nitrous oxide reduction and thus mitigates soil emissions of this greenhouse gas. *Scientific Reports*, 9(1), 20182. <https://doi.org/10.1038/s41598-019-56694-3>
- Henneron, L., Cros, C., Picon-Cochard, C., Rahimian, V., & Fontaine, S. (2019). Plant economic strategies of grassland species control soil carbon dynamics through rhizodeposition. *Journal of Ecology*, 108(2), 528–545. <https://doi.org/10.1111/1365-2745.13276>
- Henneron, L., Kardol, P., Wardle, D., Cros, C., & Fontaine, S. (2020). Rhizosphere control of soil nitrogen cycling: A key component of plant economic strategies. *New Phytologist*, 228(4), 1269–1282. <https://doi.org/10.1111/nph.16760>
- Hobbie, S. E. (2015). Plant species effects on nutrient cycling: Revisiting litter feedbacks. *Trends in Ecology & Evolution*, 30(6), 357–363. <https://doi.org/10.1016/j.tree.2015.03.015>
- Hong, S., Yin, G., Piao, S., Dybzinski, R., Cong, N., Li, X., et al. (2020). Divergent responses of soil organic carbon to afforestation. *Nature Sustainability*, 3(9), 694–700. <https://doi.org/10.1038/s41893-020-0557-y>
- Houlton, B. Z., Morford, S., & Dahlgren, R. (2018). Convergent evidence for widespread rock nitrogen sources in Earth's surface environment. *Science*, 360(6384), 58–62. <https://doi.org/10.1126/science.aan4399>
- Houlton, B. Z., Wang, Y. P., Vitousek, M. P., & Field, B. C. (2008). A unifying framework for dinitrogen fixation in the terrestrial biosphere. *Nature*, 454(7202), 327–330. <https://doi.org/10.1038/nature07028>
- IPCC. (2014). *IPCC climate change 2014: Synthesis report*, Core Writing Team, In R. K. Pachauri, & L. A. Meyer (Eds.). Retrieved from <http://ipcc.ch/report/ar5/>
- Janssen, B. H. (1996). Nitrogen mineralization in relation to C:N ratio and decomposability of organic materials. *Plant and Soil*, 181, 39–45. https://doi.org/10.1007/978-94-011-5450-5_13
- Lemma, B., Kleja, D., Nilsson, I., & Olsson, M. (2006). Soil carbon sequestration under different exotic tree species in the South-Western highlands of Ethiopia. *Geoderma*, 136(3–4), 886–898. <https://doi.org/10.1016/j.geoderma.2006.06.008>
- Li, D., Niu, S., & Luo, Y. (2012). Global patterns of the dynamics of soil carbon and nitrogen stocks following afforestation: A meta-analysis. *New Phytologist*, 195(1), 172–181. <https://doi.org/10.1111/j.1469-8137.2012.04150.x>
- Li, Y., Piao, S. L., Li, L., Chen, A. P., Wang, X. H., Ciais, P., et al. (2018). Divergent hydrological response to large-scale afforestation and vegetation greening in China. *Science Advances*, 4(5), eaar4182. <https://doi.org/10.1126/sciadv.aar4182>
- Lu, F., Hu, H., Sun, W., Zhu, J., Liu, G., Zhou, W., et al. (2018). Effects of national ecological restoration projects on carbon sequestration in China from 2001 to 2010. *Proceedings of the National Academy of Sciences of the United States of America*, 115(16), 4039–4044. <https://doi.org/10.1073/pnas.1700294115>

- Lu, X., Vitousek, P. M., Mao, Q., Gilliam, F. S., Mo, J., Turner, B. L., et al. (2021). Nitrogen deposition accelerates soil carbon sequestration in tropical forests. *Proceedings of the National Academy of Sciences of the United States of America*, 118(16), e2020790118. <https://doi.org/10.1073/pnas.2020790118>
- Luo, Y., Field, C. B., & Jackson, R. B. (2006). Does nitrogen constrain carbon cycling, or does carbon input stimulate nitrogen cycling? *Ecology*, 87(1), 3–4. <https://doi.org/10.1890/05-0923>
- Luo, Y., Su, B., Currie, W., Dukes, J., Finzi, A., Hartwig, U., et al. (2004). Progressive nitrogen limitation of ecosystem responses to rising atmospheric carbon dioxide. *BioScience*, 54(8), 731–739. [https://doi.org/10.1641/0006-3568\(2004\)054\[0731:PNLOER\]2.0.CO;2](https://doi.org/10.1641/0006-3568(2004)054[0731:PNLOER]2.0.CO;2)
- Mason, R., Craine, J., Lany, N., Jonard, M., Ollinger, S., Groffman, P., et al. (2022). Evidence, causes, and consequences of declining nitrogen availability in terrestrial ecosystems. *Science*, 376(6590), eabh3767. <https://doi.org/10.1126/science.abh3767>
- Mooshammer, M., Wanek, W., Hämmerle, I., Fuchslueger, L., Hofhansl, F., Knoltsch, A., et al. (2014). Adjustment of microbial nitrogen use efficiency to carbon: Nitrogen imbalances regulates soil nitrogen cycling. *Nature Communications*, 5(1), 3694. <https://doi.org/10.1038/ncomms4694>
- Morford, S., Houlton, B., & Dahlgren, R. (2016). Direct quantification of long-term rock nitrogen inputs to temperate forest ecosystems. *Ecology*, 97(1), 54–64. <https://doi.org/10.1890/15-0501.1>
- Nair, R., Perks, M., Weatherall, A., Baggs, E., & Mencuccini, M. (2016). Does canopy nitrogen uptake enhance carbon sequestration by trees? *Global Change Biology*, 22(2), 875–888. <https://doi.org/10.1111/gcb.13096>
- Niu, S. L., Classen, A. T., Dukes, J. S., Kardol, P., Liu, L. L., Luo, Y. Q., et al. (2016). Global patterns and substrate-based mechanisms of the terrestrial nitrogen cycle. *Ecology Letters*, 19(6), 697–709. <https://doi.org/10.1111/ele.12591>
- Peñuelas, J., Fernández-Martínez, M., Ciais, P., Jou, D., Piao, S. L., Obersteiner, M., et al. (2019). The bioelements, the elementome and the biogeochemical niche. *Ecology*, 100(5), e02652. <https://doi.org/10.1002/ecs.2652>
- Piao, S., Fang, J., Ciais, P., Peylin, P., Huang, Y., Sitch, S., & Wang, T. (2009). The carbon balance of terrestrial ecosystems in China. *Nature*, 458(7241), 1009–1013. <https://doi.org/10.1038/nature07944>
- Reed, S. C., Cleveland, C. C., & Townsend, A. R. (2011). Functional ecology of free-living nitrogen fixation: A contemporary perspective. *Annual Review of Ecology, Evolution and Systematics*, 42(1), 489–512. <https://doi.org/10.1146/annurev-ecolsys-102710-145034>
- Richter, D., Markewitz, D., Trumbore, S., & Wells, C. (1999). Rapid accumulation and turnover of soil carbon in a re-establishing forest. *Nature*, 400(6739), 56–58. <https://doi.org/10.1038/21867>
- Running, S. Q. (2015). MOD17A3H MODIS/terra net primary production yearly L4 global 500m SIN grid V006 [Dataset]. NASA EOSDIS Land Processes DAAC. <https://doi.org/10.5067/modis/mod17a3h.006>
- Sardans, J., Vallicrosa, H., Zuccarini, P., Farré-Armengol, G., Peuelas, J., Peguero, G., et al. (2021). Empirical support for the biogeochemical niche hypothesis in forest trees. *Nature Ecology & Evolution*, 5(2), 182–191. <https://doi.org/10.1038/s41559-020-01348-1>
- Scheible, W. R., Morcuende, R., Czechowski, T., Fritz, C., Stitt, M., Palacios-Rojas, N., et al. (2004). Genome-wide reprogramming of primary and secondary metabolism, protein synthesis, cellular growth processes, and the regulatory infrastructure of Arabidopsis in response to nitrogen. *Plant Physiology*, 136(1), 2483–2499. <https://doi.org/10.1104/pp.104.047019>
- Schimel, J., & Bennett, J. (2004). Nitrogen mineralization: Challenges of a changing paradigm. *Ecology*, 85(3), 591–602. <https://doi.org/10.1890/03-8002>
- Shi, S., & Han, P. (2014). Estimating the soil carbon sequestration potential of China's Grain for Green Project. *Global Biogeochemical Cycles*, 28(11), 1279–1294. <https://doi.org/10.1002/2014GB004924>
- Shi, S., Zhang, W., Zhang, P., Yu, Y., & Ding, F. (2013). A synthesis of change in deep soil organic carbon stores with afforestation of agricultural soils. *Forest Ecology and Management*, 296, 53–63. <https://doi.org/10.1016/j.foreco.2013.01.026>
- Soudzilovskaia, N., Vaessen, S., Barcelo, M., He, J., Rahimlou, S., Abarenkov, K., et al. (2020). FungalRoot: Global online database of plant mycorrhizal associations. *New Phytologist*, 227(3), 955–966. <https://doi.org/10.1111/nph.16569>
- State Forestry Administration of the People's Republic of China. (2014). *Eighth national forest resource inventory report (2009–2013)*. State Forestry Administration of the People's Republic of China.
- Vitousek, P. M., Aber, J. D., Howarth, R. W., Likens, G. E., Tilman, D. G., Schindler, D. W., et al. (1997). Human alteration of the global nitrogen cycle: Sources and consequences. *Ecological Applications*, 7(3), 739–750. [https://doi.org/10.1890/1051-0761\(1997\)007\[0737:HAOTGN\]2.0.CO;2](https://doi.org/10.1890/1051-0761(1997)007[0737:HAOTGN]2.0.CO;2)
- Vitousek, P. M., Cassman, K., Cleveland, C., Crews, T., Field, C. B., Grimm, N. B., et al. (2002). Towards an ecological understanding of biological nitrogen fixation. *Biogeochemistry*, 57/58, 1–45. <https://doi.org/10.1023/A:1015798428743>
- Vries, W. D., Reinds, G. J., Gundersen, P., & Sterba, H. (2006). The impact of nitrogen deposition on carbon sequestration in European forests and forest soils. *Global Change Biology*, 12(7), 1151–1173. <https://doi.org/10.1111/j.1365-2486.2006.01151.x>
- Vries, W. D., Solberg, S., Dobbertin, M., Sterba, H., Laubhann, D., van Oijen, M., et al. (2009). The impact of nitrogen deposition on carbon sequestration by European forests and heathlands. *Forest Ecology and Management*, 258(8), 1814–1823. <https://doi.org/10.1016/j.foreco.2009.02.034>
- Wang, B., & Qiu, L. (2006). Phylogenetic distribution and evolution of mycorrhizas in land plants. *Mycorrhiza*, 16(5), 299–363. <https://doi.org/10.1007/s00572-005-0033-6>
- Wang, X., Wang, B., Wang, C., Wang, Z., Li, J., Jia, Z., et al. (2021). Canopy processing of N deposition increases short-term leaf N uptake and photosynthesis, but not long-term N retention for aspen seedlings. *New Phytologist*, 229(5), 2601–2610. <https://doi.org/10.1111/nph.17041>
- Wei, Y., Liu, S., Huntzinger, D. N., Michalak, A. M., Viovy, N., Post, W. M., et al. (2014). NACP M5TMP: Global and North American driver data for multimodel intercomparison. [Dataset]. <https://doi.org/10.3334/ORNLDAAAC/1220>
- Xie, Z. B., Zhu, J. G., Liu, G., Cadisch, G., Hasegawa, T., Chen, C. M., et al. (2007). Soil organic carbon stocks in China and changes from 1980s to 2000s. *Global Change Biology*, 13(9), 1989–2007. <https://doi.org/10.1111/j.1365-2486.2007.01409.x>
- Xiong, Y., & Li, Q. K. (1987). *Soils in China*. Press of Sciences.
- Xu, X., Li, D. J., Cheng, X. L., Ruan, H. H., & Luo, Y. Q. (2016). Carbon: Nitrogen stoichiometry following afforestation: A global synthesis. *Scientific Reports*, 6(1), 19117. <https://doi.org/10.1038/srep19117>
- Yang, K., He, J., Tang, W., Qin, J., & Cheng, C. C. K. (2010). On downward shortwave and longwave radiations over high altitude regions: Observation and modeling in the Tibetan Plateau. *Agricultural and Forest Meteorology*, 150(1), 38–46. <https://doi.org/10.1016/j.agrformet.2009.08.004>